EFFECT OF GAS TEMPERATURE ON BREAKDOWN POTENTIAL

G. N. Dandaron, G. Yu. Dautov, and G. M. Mustafin

The breakdown voltage of a gas at temperatures up to 1130° K is described by the generalized Paschen law [1]. The applicability of Paschen's law at higher temperatures has not received much attention. The present article is devoted to this question. It presents the results of an investigation of the breakdown of a hot gas (air) at T = 500-3500° K, δ = 0.1-0.5 cm, p = 760 mm Hg between Rogowski-type tungsten electrodes. It is shown that the generalized Paschen law for the breakdown potential of air is valid up to T ≈ 2200° K. At T > 2200° K a considerable deviation from the law is observed. Thus, for example, the experimental value of U* for T = 3300° K and δ = 0.5 cm is more than four times smaller than the value predicted by Paschen's law.

Notation

δ - width of discharge gap, cm; p - gas pressure in discharge gap, mm Hg; α - first ionization coefficient, cm^{-1}; γ - second ionization coefficient; i - discharge current, A; U* - breakdown voltage (sparking potential), V; U_i - potential drop in discharge gap; V; E - electric field strength in discharge gap, V/cm; U_1 - single ionization potential of gas, V; τ ν discharge development time, sec; λ - electron mean free path, cm; T_0 - gas temperature, °K; R - resistance, ohm; f, r, y - cylindrical coordinates; n_e - electron density.

1. Description of the Experimental Apparatus. In investigating the electrical breakdown between metal electrodes in a high-temperature gas flow we heated the gas by means of a PT-49-type arc gas heater [2].

The jet of hot gas flowing out of the arc chamber has a nonuniform radial temperature distribution. To equalize this distribution we employed a water-cooled mixing chamber 4 attached to the plasma generator (Fig. 1). Air G_4 with a swirl opposite to the roation of the plasma jet was injected into the gap between the plasma generator and the mixing chamber 4 through a swirl ring. This air stream and the rotation of the jet through 90° resulted in excellent mixing. The temperature of the hot gas at the mixing chamber outlet was regulated by varying the plasma generator power and the cold air flow rate.

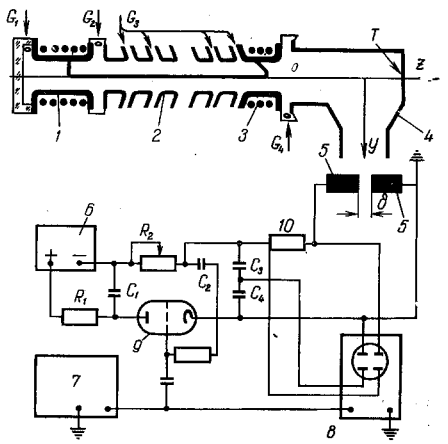

Fig. 1. Diagram of the experimental apparatus: 1,3) solenoids; 2) segment of interelectrode insert; 4) mixing chamber; 5) electrodes.

Tungsten electrodes 5 of the Rogowski type were mounted a distance δ apart symmetrically with respect to the y axis at a distance of 2 cm from the exit section of the mixing chamber nozzle. The electrode diameter was 1 cm, the diameter of the mixer nozzle outlet 2 cm.

On the interval 600-1300° K the gas temperature in the discharge gap was measured with a type TKhAP thermocouple and a MPShP1-54 secondary instrument with 0.5 accuracy calibrated to 1100° C. On the range 1300-2300° K the temperature was measured with a type OPFIR-17 optical pyrometer. For this purpose a tungsten rod, was introduced into the flow and

Novosibirsk. Translated from Zhurnal Prikladnoi Mekhaniki i Tekhnicheskoi Fiziki, Vol. 11, No. 1, pp. 138-141, January-February, 1970. Original article submitted April 16, 1969.

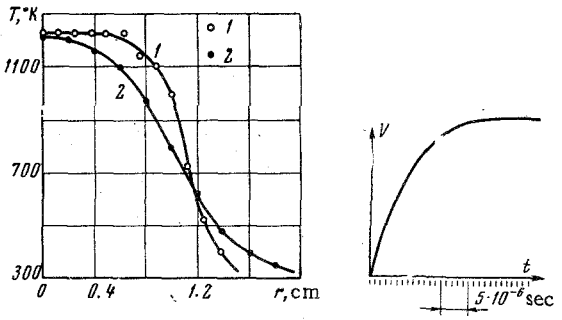

Fig. 2. Radial gas temperature distribution for different distances from the mixer nozzle exit. Curves 1 and 2 correspond to distances of 0.6 and 2 cm. Nozzle diameter 2 cm.

Fig. 3. Oscillogram of generator voltage.

the temperature determined from its luminosity. At higher values of T as the gas temperature in the discharge gap we took the mass-average stagnation temperature of the hot gas at the mixing chamber outlet, which was determined from the heat balance equation of the plasma generator-mixing chamber system.

The radial temperature distribution for two sections is presented in Fig. 2. Clearly, near the nozzle outlet the jet temperature is almost constant up to half the radius of the nozzle exit section. With distance from the nozzle exit the temperature profile becomes flatter, the reason for this being mixing of the hot jet and the surrounding cold gas. However, in the electrode section (curve 2) for $r \leq \delta_{max}/2$ ($\delta_{max} = 0.5$ cm) the temperature change does not exceed 30° K.

The working voltage was supplied to electrodes 5 from a single-pulse generator 6.

A typical oscillogram of the generator voltage pulse at i = 0 is presented in Fig. 3. The length of the pulse shoulder was regulated and had a value of the order of 10^{-5} sec. The pulse maximum was so selected that breakdown occurred on the shoulder of the pulse. In order to limit the current after breakdown and measure its value, a resistance 10 (shunt) was introduced into the circuit between the generator and the electrode. A DESO-1 double-beam oscillograph was used to record the voltage and breakdown current oscillograms.

The arc voltage and current were recorded by a class 1 M-366 voltmeter and a class 0.5 LM-1 instrument. The temperature of the cooling water was measured with mercury thermometers graduated in 0.2° C. The water and air flow rates were determined with type RS-5 and RS-7 rotameters.

2. Results of the Experiment. Oscillograms of the current i and the quantity $U' = U_l + iR$, where R is the shunt resistance, are presented in Fig. 4a. Clearly, the voltage at first increases in accordance with the external characteristic of the power source. At $U' \approx U'_{max}$ breakdown occurs, the current i begins to increase rapidly, and U_l decreases. Numerous oscillograms of U at R = 0 showed that after breakdown U_l falls sharply, almost discontinuously. The smoother decrease in U' in Fig. 4a immediately after breakdown is attributable to the rapid growth of i and hence iR. However, before breakdown i and iR are small and therefore it is possible to assume that $U^* \approx U'_{max}$. The decrease in i beyond i_{max} is a consequence of the finite capacitance of the power source capacitor. From the standpoint of a breakdown investigation the region of the oscillograms in the neighborhood of U* is of particular interest.

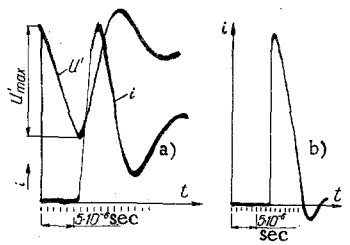

Fig. 4. Voltage and discharge current oscillograms: a) p = 760 mm Hg, δ = 0.28 mm, T = 2800° K, $\tau \sim 10^{-6}$ sec, R = 30 m; b) p = 760 mm Hg, δ = 0.28 mm, T = 300° K, $\tau \sim 10^{-6}$ sec, R = 0.

The current oscillogram for breakdown in cold air is shown in Fig. 4b. A comparison of Figs. 4a and 4b shows that as the temperature increases the rate of discharge development falls; thus, for example, at T = 300° K the discharge development time τ is of the order of 10^{-8} sec, whereas at T = 2800° K it increases to a value of the order of 10^{-6} sec. In accordance with [3], τ increases as the pressure falls. Thus, an increase in temperature has the same effect on τ as a decrease in

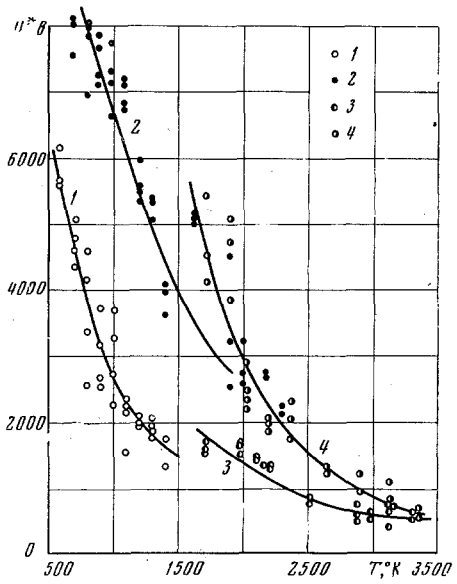

Fig. 5. Temperature dependence of the breakdown potential of air. 1,3) δ = 0.1 cm, 2,4) δ = 0.5 cm, 1,2) uncooled electrodes; 3,4) cooled electrodes.

pressure. This was to be expected, since both factors lead to a decrease in particle concentration (or gas density), which, at a given δ, as may be seen from Fig. 6, determines U*.

The temperature dependence of the breakdown potential is shown in Fig. 5 for δ = 0.1 and δ = 0.5 cm. Curves 1 and 2 were obtained for uncooled electrodes. At elevated temperatures, in order to reduce the oxidation of the tungsten, the electrodes were water-cooled (curves 3 and 4). A comparison of curves 1 and 2 with curves 3 and 4 shows that cooling the electrodes and hence reducing their temperature leads to an increase in breakdown potential. Thus, for example, at T = 1600° K, δ = 0.5 cm cooling the electrodes leads to an increase in U* by an additional ~1000 V. This effect is attributable to the role of thermionic emission and the temperature dependence of γ. On the one hand, as the electrode temperature increases, so does the current density, in accordance with the Richardson-Dushman formula [4]. In its turn, the increase in current density reduces the breakdown voltage [4]. On the other hand, owing to the increase in the kinetic energy of the electrons in the metal γ processes are intensified, i.e., the ions striking the cathode are capable of knocking out secondary electrons at lower energies.

It is clear from Fig. 5 that at small T, as the temperature increases, U* falls rapidly, and in the range investigated U* is approximately inversely proportional to T. With further increase in T the dependence of U* on T and δ becomes weaker.

It should be noted that the values of U* for cooled electrodes in Fig. 5 should be regarded as exaggerated, since the layer of relatively cold gas adjacent to the electrodes leads to an increase in U*. Therefore at temperatures above 1600° K a more rapid decrease in U* with rise in temperature is to be expected.

As the gas temperature increases, despite the cooling of the electrodes, their surface temperature rises. Consequently, at high temperatures thermionic emission may be expected to affect U* even when the electrodes are cooled.

In Fig. 6 the results obtained are compared with the generalized Paschen law [3]

$$U^* = \frac{Bp\delta T_0 / T}{B + \ln (p\delta T_0 / T)} \qquad (1)$$

where $C = \ln\left[\frac{A}{\ln(1 + 1/\gamma)}\right]$, $T_0 \approx 300°K$, $\gamma = 10^{-2}$ [3],

$$A = 15 \frac{1}{\text{cm} \cdot \text{mm Hg}}, \quad B = 365 \frac{b}{\text{cm} \cdot \text{mm Hg}} \quad [1, 3, 4].$$

In Fig. 6 Paschen's law (1) is represented by a solid line. The experimental points 5 were taken from [1] for the case T = T_0, p = 760 mm Hg, while the points 4 were obtained by the authors under the same conditions. The figure also includes the experimental data obtained for different values of T and δ. Clearly, up to T ≈ 2000-2200° K the experimental data are satisfactorily described by the generalized Paschen law (1). However, at T > 2200° K there is a substantial deviation from Paschen's law, and the experimental data become stratified. Thus, for example, the experimental value of U* for T = 3300° K and δ = 0.5 cm is more than four times smaller than the value predicted by Paschen's law.

We will consider the possible reasons for the deviation of the experimental data from (1). The constants entering into (1) were obtained from the experimental data on breakdown in a stationary gas. In our

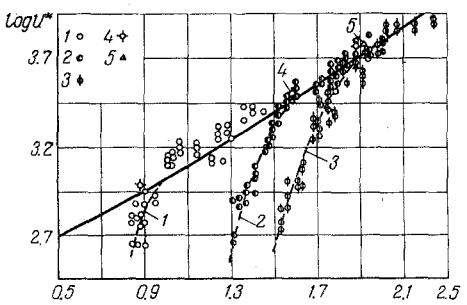

Fig. 6. Breakdown voltage as a function of the parameter $p\delta T_0/T$. Curves 1, 2, and 3 correspond to δ = 0.1, 0.3, 0.5 cm, p = 760 mm Hg; 4) T = 300° K, δ = 0.1-0.5 cm, p = 760 mm Hg, 5) T = 300° K, p = 760 mm Hg, δ = 0.05-0.1 cm [1].

case breakdown takes place in a gas flow in the presence of a pulsed voltage. Equation (1) was obtained from the continuity equation for an electron gas, which may be written in the dimensionless form

$$\frac{\partial n_e}{\partial t} + \frac{v_{y0}\tau}{\delta}\frac{\partial}{\partial y}(n_e v_y) + \frac{v_{r0}\tau}{\delta}\frac{\partial}{\partial r}(r n_e v_r) + \frac{v_{\varphi 0}\tau}{\delta r}\frac{\partial}{\partial \varphi}(n_e v_\varphi) = \alpha r n_e v_{e0}|v_e|. \quad (2)$$

Here ν_{y0}, v_{r0}, $v_{\varphi 0}$ are the characteristic values of the electron velocity components along the coordinate axes (Fig. 1). We will estimate the ratio of the coefficients $v_{y0}\tau/\delta$ and $v_{r0}\tau/\delta$. As v_{y0} we take the experimental gas flow velocity, which was of the order of 10^4 cm/sec, and as v_{r0} the electron drift velocity in the electric field. At $E = 4 \cdot 10^3$ V/cm, using the data of [3], we find $v_{r0} \sim 10^6$ cm/sec and $v_{y0}/v_{r0} \ll 1$. Thus, it is possible to neglect the term $v_{y0}\tau\delta^{-1}\,\partial\,(n_e v_y)/\partial y$, which takes into account the effect of the motion of the gas on the breakdown processes, as compared with the other terms. Physically, this means that during breakdown the motion of the gas $v_{y0}\tau$ is very small as compared with the motion of the electrons $\delta = v_{r0}\tau$, and therefore under the experimental conditions described the gas may be assumed stationary.

The data of [1] show that if the pulse rises at a rate of $9.3 \cdot 10^{11}$ V/sec and the width of the discharge gap δ = 12 cm, the pulse breakdown voltage differs from the static breakdown voltage by 2-4%. This difference decreases with decrease in the width of the discharge gap and the pulse rise rate. In the experiments the latter rate and the value of δ did not exceed 10^8 V/sec and 0.5 cm, respectively, and the effect of the pulsed nature of the voltage on U* can be neglected. Thus, there must be other reasons for the deviation of the experimental data from Paschen's law. Apparently, the following factors are responsible. Firstly, at T $\approx$ 2200° K intense dissociation of the oxygen and nitrogen molecules, the formation of NO, etc. begins. Naturally, the change in gas composition leads to a change in the physical properties of the gas. Thus, for example, the effective ionization potential of air is 14.5 V, while the ionization potential of NO is only 9.5 V [3]. NO also has a higher value of the electron impact ionization cross section than N_2 and O_2. Secondly, as the temperature increases, the concentration of excited particles increases in accordance with the Boltzmann distribution. This, in turn, causes an increase in the efficiency of cumulative ionization. Since cumulative ionization requires less energy than ionization from the ground state, as T increases an ever greater number of electrons becomes capable of ionizing particles. These factors tending to reduce the breakdown voltage are not taken into account in Townsend's theory or Paschen's law.

Thus, as a result of our investigations we have established that the breakdown voltage for air at T $\leq$ 2200° K and p = 1 atm abs can be calculated on the basis of the generalized Paschen law. At higher temperatures Paschen's law is violated. In this case our experimental data can be used to estimate the breakdown potential of air on the interval 2000-3500° K.

LITERATURE CITED

1. J. Meek and J. Craggs, Electrical Breakdown of Gases [Russian translation], IL, Moscow, 1960.
2. G. M. Mustafin, "Characteristics of a stabilized arc in a channel with a distributed gas supply," PMTF [Journal of Applied Mechanics and Technical Physics], no. 4, 1968.
3. A. von Engel, Ionized Gases [Russian translation], Fizmatgiz, Moscow, 1959.
4. N. A. Kaptsov, Electrical Phenomena in Gases and Vacuum [in Russian], Gostekhteoretizdat, Moscow-Leningrad, 1947.